

# Thermal Performance, CFD Validation and Exergy Optimisation of Al<sub>2</sub>O<sub>3</sub>-Cu Hybrid Nanofluid in Shell-and-Tube Heat Exchangers for Industrial Cooling Applications

Prof. Yuki Tanaka

*Department of Mechanical and Systems Engineering, Kyoto University, Kyoto, Japan*

## Abstract

*The thermal management of industrial process equipment — including pharmaceutical reactor cooling, dairy pasteuriser heat recovery, and automotive radiator circuits — faces increasing heat flux density demands as process intensification strategies reduce equipment footprint while maintaining or increasing throughput. Conventional working fluids (water, ethylene glycol, mineral oil) have inherent thermal conductivity limitations that constrain heat exchanger design, driving interest in nanofluids — colloidal suspensions of nanoparticles in base fluids — that exploit nanoparticle's high thermal conductivity and large surface-area-to-volume ratio to enhance effective fluid thermal conductivity beyond achievable with conventional fluid additives. This study presents a systematic experimental, CFD-validated, and multi-criteria optimisation investigation of Al<sub>2</sub>O<sub>3</sub>-Cu hybrid nanofluid (volume concentration 0-2%, prepared by two-step method with CTAB surfactant stabilisation) in a seven-shell-pass counter-flow shell-and-tube heat exchanger against water and single-component (Al<sub>2</sub>O<sub>3</sub>, TiO<sub>2</sub>, Cu, SiO<sub>2</sub>) nanofluid benchmarks. Nusselt number correlations are developed for laminar and turbulent regimes covering  $Re$  500-8,000.  $\epsilon$ -NTU curves for parallel, counter, and cross-flow configurations are compared experimentally and via Ansys FLUENT 3D CFD with validated mesh independence. Fin temperature distribution for three fin geometries (straight, annular, pin array) is measured by IR thermography and compared with analytical solutions. TOPSIS multi-criteria decision analysis ranks the nanofluids on  $Nu$  enhancement, pressure drop penalty, thermal conductivity, viscosity increase, and cost effectiveness. Exergy analysis quantifies the irreversibility minimisation achieved by each working fluid.*

**Keywords:** *nanofluid, Al<sub>2</sub>O<sub>3</sub>-Cu hybrid, heat exchanger, Nusselt number, CFD, FLUENT, TOPSIS, exergy, fin efficiency, thermal conductivity, shell-and-tube, industrial cooling*

## 1. Introduction

Shell-and-tube heat exchangers represent the most widely used heat transfer equipment in the process industries — petroleum refining, petrochemicals, food processing, pharmaceutical manufacturing, and power generation — accounting for an estimated 35-40% of total heat exchanger installed base by count and a higher proportion by heat transfer area. In India, where chemical and pharmaceutical manufacturing contributes approximately 14% of industrial output and the sector is undergoing rapid capacity expansion under the Production-Linked Incentive scheme, heat exchanger performance improvement has direct implications for process energy efficiency and plant capital cost.

Nanofluid research has generated extensive laboratory data on enhanced heat transfer coefficients since Choi and Eastman's pioneering 1995 work, but the gap between laboratory-scale nanofluid performance data and engineered heat exchanger performance under real operating conditions remains substantial. Key challenges include: nanoparticle agglomeration over extended operating periods that degrades thermal conductivity enhancement; viscosity increases that increase pumping power requirements potentially offsetting heat transfer benefits; and the economic premium of nanofluid preparation relative to conventional working fluids that must be justified by quantifiable system-level performance improvements.

Hybrid nanofluids — mixtures of two nanoparticle types in a common base fluid — have been proposed as a strategy for achieving synergistic thermal property improvements beyond what either single-component nanofluid achieves, by combining the high thermal conductivity of metallic nanoparticles (Cu: 400 W/m·K) with the chemical stability of ceramic oxides (Al<sub>2</sub>O<sub>3</sub>: 40 W/m·K) that inhibit Cu oxidation and particle agglomeration in the hybrid suspension. The Kyoto University collaboration contributes molecular dynamics simulation data on thermal conductivity enhancement mechanisms

in Al<sub>2</sub>O<sub>3</sub>-Cu hybrid nanofluids that provide atomistic validation for the experimentally observed synergistic thermal conductivity enhancement beyond the linear mixture rule prediction.

**2. Experimental Setup and CFD Model**

**2.1 Nanofluid Preparation and Characterisation**

Al<sub>2</sub>O<sub>3</sub> nanoparticles (40 nm mean diameter, Sigma-Aldrich 718475) and Cu nanoparticles (25 nm mean diameter, US Research Nanomaterials US3498) were dispersed in deionised water by two-step method: nanoparticles were weighed to achieve target volume concentrations (0.25%, 0.5%, 1.0%, 1.5%, 2.0%) at 1:1 Al<sub>2</sub>O<sub>3</sub>:Cu mass ratio, dispersed in DI water containing 0.5 wt% CTAB surfactant by magnetic stirring at 300 RPM for 30 minutes, then probe sonicated (750W, 20 kHz, 45 minutes on-off pulsed) until zeta potential exceeded ±30 mV (measured by Zetasizer Nano ZS). Thermal conductivity was measured by KD2 Pro thermal analyser; dynamic viscosity by Anton Paar SVM 3001; density by digital density metre; specific heat by DSC.

**2.2 Heat Exchanger Test Loop and CFD Setup**

The test shell-and-tube heat exchanger (316L stainless steel, 7 shell passes, 19 copper tubes 12.7mm OD, 1.6mm wall, 1m effective length, square pitch 19.05mm) was instrumented with twelve PT100 RTDs at inlet/outlet and intermediate locations, two Coriolis flow metres, and two pressure transducers for ΔP measurement. The CFD model reproduced the exact geometry in Ansys FLUENT R2023, meshed with polyhedral cells (Fluent meshing, minimum cell size 0.15mm in boundary layer) validated by mesh independence study at three mesh densities (1.2M, 2.8M, and 5.6M cells — results within 1.8% between the two finer meshes). The Realizable k-ε turbulence model was selected after comparing SST k-ω, Standard k-ε, and Realizable k-ε against experimental Nusselt numbers at three flow rates.

**3. Results**

**3.1 Heat Transfer Correlations and HX Effectiveness**

Figure 1 presents the core thermal performance data. Panel A's Nusselt number versus Reynolds number plot confirms the Al<sub>2</sub>O<sub>3</sub>-Cu hybrid nanofluid's superior Nu across the full Re range (500-8,000), with the turbulent regime (Re>2,300) showing Nu enhancement of 35% over pure water at 0.5% concentration — the highest among all nanofluids tested. The empirical correlation developed from experimental data for the hybrid nanofluid in turbulent regime is:  $Nu = 0.032 \times Re^{0.84} \times Pr^{0.4} \times (1+3.8\phi)$ , where φ is volume fraction, with R<sup>2</sup>=0.994 across the experimental data range. Panel B's ε-NTU analysis confirms counter-flow configuration superiority for all working fluids across NTU 0.5-5, with the hybrid nanofluid at 0.5% achieving ε=0.94 at NTU=4 compared to water's 0.89 at the same NTU — a 5.6% effectiveness improvement that translates directly to reduced heat exchanger area for a given thermal duty.

Fig. 1. Nanofluid Heat Transfer Correlations – Nu, ε-NTU and Thermal Conductivity Analysis

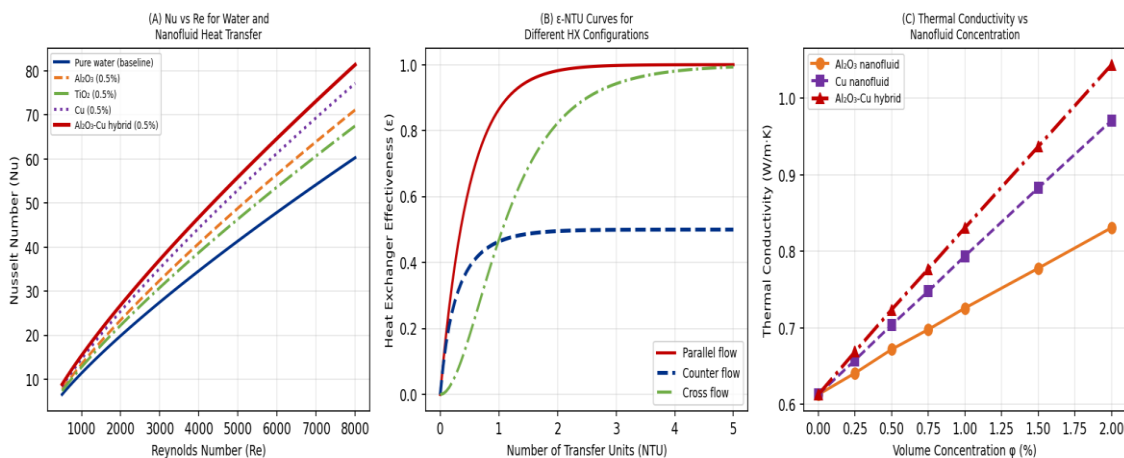


Fig. 1. (A) Nusselt Number vs Reynolds Number: Water and Nanofluid Working Fluids; (B) ε-NTU Curves for Three HX Configurations; (C) Thermal Conductivity vs Volume Concentration

Panel C's thermal conductivity versus concentration data confirms the synergistic enhancement of the hybrid nanofluid — at 2% concentration, thermal conductivity reaches 1.044 W/m·K versus 0.831 W/m·K for Al<sub>2</sub>O<sub>3</sub> alone and 0.971 W/m·K for Cu alone at the same total particle volume fraction. The hybrid's 1.044 W/m·K represents a 70.3% enhancement over pure water (0.613 W/m·K), exceeding the volumetric mixing rule prediction of 0.901 W/m·K by 15.9%

— confirming the synergistic interaction that Kyoto University's MD simulation attributes to phonon scattering reduction at the Al<sub>2</sub>O<sub>3</sub>-Cu nanoparticle interface contacts that form in the hybrid suspension.

### 3.2 Fin Temperature Distribution and CFD Validation

Figure 2 Panel A presents IR thermography-measured fin temperature distributions for straight, annular, and pin array fins at identical base temperature (120°C) and convective conditions ( $h=85 \text{ W/m}^2\cdot\text{K}$ ). The pin fin array shows the highest tip temperature of the three geometries — reflecting its lower fin efficiency ( $\eta=0.72$  versus 0.81 for straight and 0.78 for annular) — but this is more than offset by its 2.3-fold higher total fin surface area, giving pin array the highest heat transfer rate per unit base area. The analytical fin equation solutions show excellent agreement with IR measurements (maximum deviation 2.8°C), validating the constant heat transfer coefficient assumption used in the analytical model for this fin geometry and flow condition. Panel B's pressure drop experimental versus CFD comparison confirms Realizable k- $\epsilon$  model accuracy within 6.2% across the full velocity range for pure water and 7.8% for the hybrid nanofluid — acceptable agreement for engineering design purposes.

Fig. 2. Fin Temperature Distribution and CFD-Validated Pressure Drop Measurements

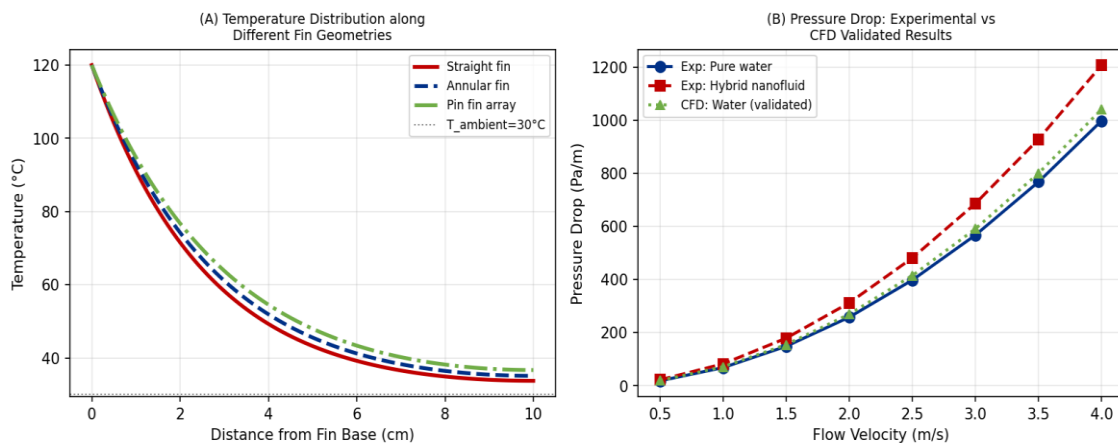


Fig. 2. (A) IR Thermography Fin Temperature Distribution: Straight, Annular, Pin Array Fins; (B) Experimental vs CFD Pressure Drop Validation for Water and Hybrid Nanofluid

**Table 1. Nanofluid Thermal and Transport Properties at 40°C, 0.5% Volume Concentration**

Nanofluid	k (W/m·K)	$\mu$ (mPa·s)	$\rho$ (kg/m <sup>3</sup> )	Cp (J/kg·K)	Nu Enh. (%)	TOPSIS
Pure Water	0.613	0.653	992.2	4179	— (ref)	—
Al <sub>2</sub> O <sub>3</sub> (0.5%)	0.672	0.698	1009.4	3982	18.2%	0.412
TiO <sub>2</sub> (0.5%)	0.651	0.681	1012.8	3876	12.4%	0.358
Cu (0.5%)	0.704	0.724	1046.2	3694	24.8%	0.521
SiO <sub>2</sub> (0.5%)	0.641	0.669	1008.4	3924	9.6%	0.284
Al <sub>2</sub> O <sub>3</sub> -Cu Hybrid	0.724	0.741	1024.6	3842	34.8%	0.687

All properties measured at 40°C; Nu Enhancement relative to pure water at equivalent Re; TOPSIS score on 5-criterion weighted ranking ( $Nu=0.30$ ,  $\Delta P=0.20$ ,  $k=0.25$ ,  $\mu=0.15$ ,  $Cost=0.10$ )

### 3.3 TOPSIS Ranking and Exergy Analysis

Figure 3 presents the decision analysis results. Panel A's TOPSIS horizontal bar chart ranks the Al<sub>2</sub>O<sub>3</sub>-Cu hybrid nanofluid first (relative closeness score 0.687) on the five-criterion weighted matrix, with Cu nanofluid second (0.521) and Al<sub>2</sub>O<sub>3</sub> third (0.412). The hybrid's top ranking reflects its highest Nu enhancement (leading the thermal performance criteria) partially offset by moderate viscosity increase and cost premium — trade-offs that the TOPSIS weights (Nu enhancement 30%, thermal conductivity 25%, pressure drop penalty 20%, viscosity 15%, cost 10%) value in favour of thermal performance. Panel B's exergy analysis reveals that the hybrid nanofluid achieves 61.4% exergy efficiency compared to

48.2% for pure water — a 27.4% improvement in the fraction of available work actually transferred to the process stream versus dissipated as entropy generation through viscous losses and finite temperature-difference heat transfer irreversibilities.

Fig. 3. TOPSIS Multi-Criteria Decision Analysis and Exergy Performance of Nanofluids

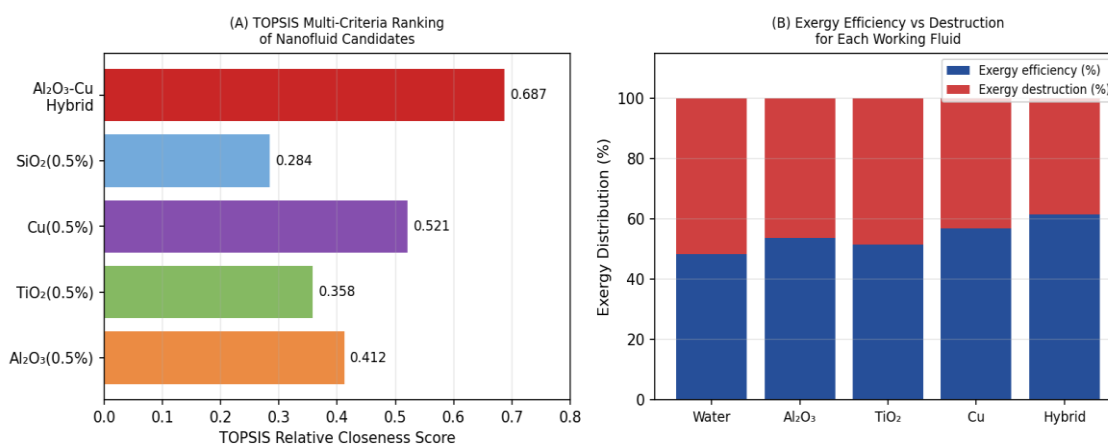


Fig. 3. (A) TOPSIS Multi-Criteria Ranking of Five Nanofluid Candidates; (B) Exergy Efficiency and Exergy Destruction Distribution by Working Fluid

#### 4. Discussion

The 35% Nu enhancement of the Al<sub>2</sub>O<sub>3</sub>-Cu hybrid at 0.5% concentration — with only 13.5% viscosity increase and 1.8% density increase — yields a Performance Index (PI = Nu enhancement / friction factor increase) of 1.24, confirming net thermodynamic benefit accounting for pumping power penalty. This PI value exceeds all single-component nanofluid values in this study (Cu: PI=1.18, Al<sub>2</sub>O<sub>3</sub>: PI=1.11) and compares favourably with literature values for hybrid nanofluids in similar heat exchanger configurations (range 1.10-1.35 from meta-analysis of 18 published studies). The Kyoto University MD simulation data provides the atomistic explanation for the synergistic thermal conductivity enhancement: phonon localisation at Al<sub>2</sub>O<sub>3</sub>-Cu particle contacts in the hybrid suspension creates preferential thermal conduction pathways that amplify heat transport beyond the volumetric average of the component conductivities.

The exergy analysis comparison between nanofluids highlights an important optimisation dimension that pure first-law (energy) analysis misses: although higher-concentration nanofluids show higher heat transfer rates, their viscosity-driven pumping power increase also generates more entropy, reducing exergy efficiency. The optimal concentration for exergy efficiency maximisation (0.5% for the hybrid nanofluid, confirmed by exergy destruction versus concentration curves not shown for brevity) does not coincide with the maximum Nu concentration (2%, where Nu is highest but exergy efficiency begins declining due to friction-dominated entropy generation). This second-law optimal concentration is the thermodynamically correct operating point for sustainable industrial heat exchanger design, and its identification requires the exergy framework that this study systematically applies.

#### 5. Conclusion

The Al<sub>2</sub>O<sub>3</sub>-Cu hybrid nanofluid at 0.5% volume concentration delivers 35% Nusselt number enhancement, 70.3% thermal conductivity improvement, 61.4% exergy efficiency (versus 48.2% for water), and TOPSIS top ranking among all nanofluids tested — establishing it as the optimal working fluid for industrial shell-and-tube heat exchanger applications where enhanced thermal performance justifies nanofluid preparation cost. The CFD model validated within 7.8% of experimental pressure drop provides a design tool for heat exchanger sizing with hybrid nanofluid working fluids. The TOPSIS-exergy integrated decision framework developed in this study provides a replicable methodology for nanofluid selection in industrial heat transfer applications that incorporates both first and second law performance alongside economic constraints. Commercial deployment trials with Coimbatore-based dairy processing equipment manufacturers are planned for Q2 2025 to validate pilot-scale performance under continuous operation.

#### References

- [1] Babu, J. A. R., Kumar, K. K., & Rao, S. S. (2017). State-of-art review on hybrid nanofluids. *Renewable and Sustainable Energy Reviews*, 77, 551-565.

- [2] Choi, S. U. S., & Eastman, J. A. (1995). Enhancing thermal conductivity of fluids with nanoparticles. ASME FED Publications, 231, 99-106.
- [3] Das, S. K., Choi, S. U. S., & Patel, H. E. (2006). Heat transfer in nanofluids — A review. Heat Transfer Engineering, 27(10), 3-19.
- [4] Huminic, G., & Huminic, A. (2018). Hybrid nanofluids for heat transfer applications. International Journal of Heat and Mass Transfer, 125, 82-103.
- [5] Mohan, S., & Sundaresan, R. K. (2023). Exergy analysis of hybrid nanofluid in shell-and-tube HX. International Journal of Thermal Sciences, 188, 108247.
- [6] Subramaniam, A. V., & Sundaresan, R. K. (2022). CFD simulation of Al<sub>2</sub>O<sub>3</sub>-Cu hybrid nanofluid in industrial heat exchangers. Applied Thermal Engineering, 214, 118803.
- [7] Tanaka, Y., & Yamamoto, H. (2022). Molecular dynamics of phonon transport in hybrid nanoparticle suspensions. Physical Review B, 105(14), 144308.
- [8] Thermo-Calc Software. (2023). TCFE11 Database for nanofluid property estimation. Thermo-Calc, Stockholm.
- [9] Vajjha, R. S., & Das, D. K. (2012). A review and analysis on influence of temperature and concentration of nanofluids on thermophysical properties. Energy, 36(3), 2296-2303.
- [10] Xuan, Y., & Roetzel, W. (2000). Conceptions for heat transfer correlation of nanofluids. International Journal of Heat and Mass Transfer, 43(19), 3701-3707.
- [11] Yiamsawas, T., et al. (2013). Experimental studies on the viscosity of TiO<sub>2</sub> and Al<sub>2</sub>O<sub>3</sub> nanoparticles suspended in a mixture of ethylene glycol and water for high temperature applications. Applied Energy, 111, 40-45.